Investigating Nonlinear Modal Energy Transfer in a Random Load Environment

Joseph D. Schoneman[1] **and Matthew S. Allen**[2]

[1] Graduate Student; e-mail: schoneman@wisc.edu

[2] Assistant Professor; e-mail: matt.allen@wisc.edu

University of Wisconsin — Department of Engineering Physics

1500 Engineering Drive

Madison, WI 53706

Abstract

When a structure is subjected to an extreme environment, its linear normal modes, which are uncoupled under small loads, begin to influence each other and exchange energy. This is easily explained when the nonlinear normal modes of the structure are computed, since they show internal resonances where the underlying linear modes combine to produce the NNM solution at each excitation level. This paper examines the degree to which nonlinear modal coupling can serve as an energy transfer mechanism in order to reduce the vibration levels of a structure subjected to a broadband, random forcing. The structure in question is a beam with an intermediate support that is adjusted in order to vary the frequency ratios between modes. To explore the significance of modal coupling, two types of reduced order models are examined: A customary model including all of the coupling terms between the linear modes, and an uncoupled reduced order model which contains nonlinear stiffness terms in single modes only. The differences in response between the two models are used to quantify the effect of nonlinear modal coupling in the structure.

Keywords: Nonlinear Reduced Order Modeling, Nonlinear Normal Modes, Random Response

1 INTRODUCTION

Linear analysis techniques are the foundation of modern structural dynamics. Most structures behave linearly at low levels of dynamic excitation, but certain high performance applications require a combination of low structural weight and high environmental loads, causing responses in the nonlinear regime. Specific motivating cases include skin panels of hypersonic vehicles[1], which undergo severe thermo-acoustic loadings at cruising speeds in excess of Mach 5, as well as the ducted engine assemblies of stealth aircraft, where jet exhaust impinges directly on the structure. Geometric nonlinearity is also prevalent in the design of joined-wing concepts[2], and in the behavior of extremely lightweight space structures such as solar sails[3].

It has long been possible to compute the response of geometrically nonlinear structures in finite element software, but the computational cost is orders of magnitude higher than that for linear analysis of the same structure. State-of-the-art finite element software combined with high performance computing clusters allow for multi-physics simulations with extremely complicated models - millions of degrees of freedom - in a reasonable amount of time: several hours to several days, depending on the model complexity and physics involved. This capability is extremely powerful, but such analysis times still limit the amount of design insight which can be obtained from a model. For applications requiring hundreds or thousands of analyses, such as optimization studies, day-long simulation times are not acceptable. Another application of interest is the “digital twin” concept under examination by the United States Air Force, which proposes the simulation of an entire aircraft over its flight history in

near-real-time[4]. Full-order coupled simulation of the thermal, aerodynamic, and nonlinear structural physics of an aircraft is still barely (if at all) feasible, let alone achievable in real-time.

One key strategy for addressing these concerns is the use of reduced order modeling (ROM) or, more specifically, nonlinear reduced order modeling (NLROM) techniques. Over the past three decades, NLROM techniques have emerged which allow efficient simulation of geometric nonlinearity in beams and plates experiencing large deformations relative to their thickness. This type of nonlinearity occurs due to the axial "membrane" stretching when thin members deflect on the order of their thickness; a schematic is given for a clamped-clamped beam in Figure 1.

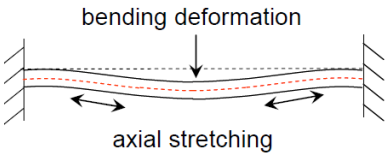

Figure 1: *Illustration of axial stretching effects for a clamped-clamped beam. At low deflections, deformation along the neutral axis is negligible; as the deflection increases towards one beam thickness, the axial deformation increases nonlinearly and must be included in the analysis.*

The earliest known presentation of NLROM techniques is that by Nash[5], with other early work in the field put forward by Segalman & Dorhmann[6][7], McEwan[8], and Muravyov & Rizzi[9]. A review of work in the field was performed by Mignolet et al.[10] in 2013. Nonlinearities are almost always represented as a series of quadratic and cubic terms in the modal coordinates, which are usually obtained by leveraging the nonlinear analysis capabilities of commercial finite element (FE) software. A low-order subset (usually below ten) of linear modes is selected for inclusion in the NLROM; a series of static (FE) analyses then characterizes the nonlinear effects of membrane stretching. Forces (or deflections) are applied in the shapes of the selected modal basis, and the resulting deflections (or forces) from the finite element analysis are used to determine suitable coefficients for nonlinear terms in the NLROM. The technique used for this study is given by Gordon & Hollkamp in[1] and[11], and described in further detail in Section 3.1.

While quite a few works have discussed how to compute accurate and efficient NLROMs, little has been done to explore how these techniques can be leveraged for to optimize the design of a structure. However, several works have explored optimization of geometrically nonlinear structures. With energy harvesters as a target application, Dou & Jensen seek to maximize the response of a nonlinear beam at resonance[12]; focusing on nonlinear tuned vibration absorbers, which maintain robustness in the presence of base structure nonlinearity, Grappasonni describes an optimization process used to match the characteristics of a tuned nonlinear vibration absorber to the nonlinearity of the base structure [13]. In these works the Galerkin method was used to create simple low-order models of the structures of interest; higher fidelity finite element models were not considered.

Structural loads during hypersonic flight regimes can be represented as broadband, random forcings. Random response computations are a particularly attractive use of NLROMs due to the long time histories required to obtain response statistics in a nonlinear model and the ensuing high computational costs of a full-order model. There are two key mechanisms which may reduce (or increase) the response level of a structure relative to a linear analysis:

- As displacements increase, the structure stiffens as a result of membrane stretching. This is primarily a static effect.
- Coupling between nonlinear normal modes - discussed in Section 3.3 - transfers energy from excited modes to non-excited modes. Often, lower frequency modes will transfer energy to higher frequency modes acting to increase the effective damping of some modes; however, this can also cause unexpected response levels at higher frequencies.

A parallel study[14] examined the weight reduction achievable in a simple beam using a single-mode model and considering only the stiffening behavior mentioned above. In contrast, the objective of this study is to examine specifically the reduction in response which results from nonlinear modal coupling. It is difficult to precisely decouple the effects of increased stiffness and the effects of modal energy transfer, but as a proxy, the response of fully coupled NLROMs is compared with that predicted by uncoupled NLROMs. Using the efficient analysis capability of these NLROMs, the structural response over a range of parameters is examined in a two-dimensional design space, in order to better understand the topology of the stress and displacement response surfaces.

A key concept in the analysis of nonlinear structures is that of the nonlinear normal mode, a generalization of the linear normal mode to nonlinear structures. The NNM concept in use here defines a nonlinear normal mode as a *not-necessarily synchronous periodic response of the conservative nonlinear system*[15]; since the system is nonlinear, its periodic response is a function of the amplitude of its state variables. Both the frequency of the periodic response and its shape evolve based on the amplitude of these variables.

A common visualization for the NNM is the frequency-energy plot (FEP), which tracks the variation of the resonant frequency as a function of energy present in the structure - see Figure 5 for an example. FEP's allow an easy understanding of the basic characteristics of a nonlinear system and also allow ready identification of any "internal resonances" present in the system. These resonances typically occur when a lower mode's frequency reaches an integer multiple of a higher mode's frequency, and it is theorized that they may play a significant role in modal energy transfer. In much of the classical literature (see, e.g. Nayfeh[16]) internal resonances occur only when the linear natural frequencies have certain ratios. In the NNM framework, they may also occur as the frequency of one NNM backbone becomes a multiple of another NNM backbone. By adjusting the ratio of linear natural frequencies, the energy level at which an internal resonance appears can be adjusted.

The framework of the paper is as follows: First, the structure and load case of interest are described, and a reference condition is developed using linear analysis techniques. The NLROM technique in use is then described, and full-order simulations of the model are generated and compared to reduced-order results. Finally, a two-dimensional parameter sweep is performed in order to visually examine the response of the structure as a function of the varied parameters. The accuracy of fully coupled and uncoupled NLROM's is compared, and a hypothetical optimum is chosen for the model. A discussion of the results and their implications follows.

2 EXAMPLE STRUCTURE AND LINEAR ANALYSIS

The structure of interest for this study is a clamped-clamped beam with an intermediate support. The intermediate support is constrained vertically but left free in the horizontal and rotational coordinates; a schematic is shown in Figure 2. The location of this support can be adjusted to modify the ratios of natural frequencies in the model. These ratios determine the location in frequency-energy space of any internal resonances in the structure. All of the simulations presented in this study use a uniform pressure loading applied to the left half of the beam; the pressure amplitude is a broadband, random variable with a flat power spectral density (PSD) level from 0 to 1000 Hz. The half-beam, rather than a full-beam, loading is used in order to spatially excite as many modes of the structure as possible and to break the symmetry of the configuration.

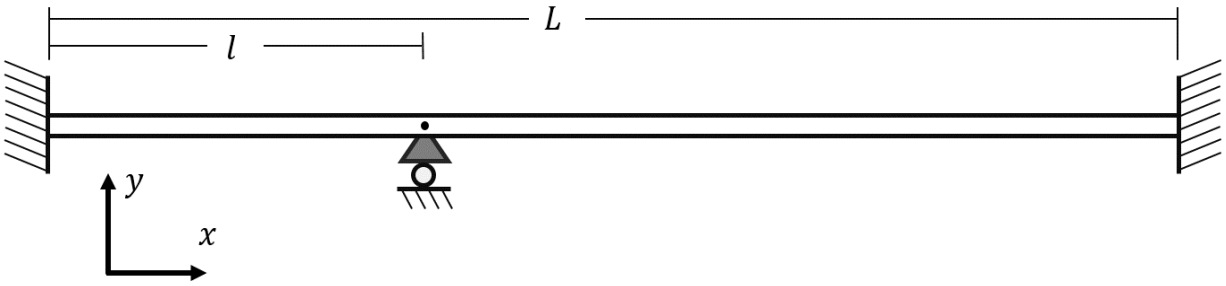

Figure 2: *A schematic of the beam under consideration for the present study.*

In addition to affecting the natural frequency ratios, adjusting the support location also adjusts the bending stiffness of the beam with respect to a given loading. As such, only beam configurations which are near the maximum-stiffness support ratio location will be examined. This location can be determined using traditional linear structural dynamics techniques. A "reference beam" is used for this calculation, with properties given in Table 1.

To obtain a structural model of the beam, a MATLAB-based beam finite element tool is used to generate mass and stiffness matrices; the response of the structure is then calculated in the modal domain. The process is briefly demonstrated below. The

Thickness [mm]	Length [mm]	Width [mm]	Young's Modulus [MPa]	Density [$\mathrm{Tonne}/\mathrm{mm}^3$]
2	250	25	$71,000$	$2.7 \cdot 10^{-9}$

Table 1: Properties of the beam used for linear support optimization.

equations of motion for a linear structure with n degrees of freedom are

$$\mathbf{M}\ddot{\mathbf{x}} + \mathbf{C}\dot{\mathbf{x}} + \mathbf{K}\mathbf{x} = \mathbf{f} \tag{1}$$

with $\mathbf{M}$, $\mathbf{C}$, and $\mathbf{K}$ the respective mass, damping, and stiffness matrices (all size $n \times n$), $\mathbf{x}$ the displacements of the structure, $\mathbf{f}$ the vector of applied forces, (both size $n \times 1$), and the overdot representing a derivative with respect to time. The structure's linear normal modes are obtained by performing a coordinate transformation $\mathbf{x} = \mathbf{\Phi q}$ in which $\mathbf{q}$ are "modal coordinates" representing the response level of the normal modes which are contained in the columns of the modal matrix $\mathbf{\Phi}$. The modes themselves are found by solving the generalized eigenvalue problem for the undamped structure,

$$[\mathbf{K} - \omega_r^2 \mathbf{M}]\phi_r = 0 \tag{2}$$

in which each eigenvector ϕ_r corresponds to a circular natural frequency ω_r. The modal matrix is normalized such that it is orthogonal with respect to the mass matrix, i.e. $\mathbf{\Phi}^T\mathbf{M}\mathbf{\Phi} = \mathbf{I}$; this also requires that $\mathbf{\Phi}^T\mathbf{K}\mathbf{\Phi} = \mathbf{\Lambda}$ where $\mathbf{\Lambda}$ is a diagonal matrix with $\Lambda_{rr} = \omega_r^2$. Taking all this together, the equation of motion (1) becomes

$$\ddot{\mathbf{q}} + \bar{\mathbf{C}}\dot{\mathbf{q}} + \mathbf{\Lambda q} = \mathbf{\Phi}^T\mathbf{f} \tag{3}$$

The modal damping matrix is specified using critical damping ratios for each mode such that $\bar{C}_{rr} = 2\zeta_r\omega_r$. A ratio of 0.01% is used throughout this work for all modes.

It is usually not practical or necessary to retain all n linear normal modes for simulation of a linear response. By considering only a subset m of dynamically important modes, a linear reduced order model (ROM) is created. Selection of dynamically important modes is performed by considering the frequency content of the loading; in this case, with no excitation above 1000 Hz, the first four modes of the structure are included: For the properties given above, the lowest possible fourth bending mode has a natural frequency of 1507 Hz.

Finally, the linear response to a random excitation is considered. The frequency-domain solution to Equation (3) is

$$\mathbf{Q} = [-\omega^2\mathbf{I} + i\omega\bar{\mathbf{C}} + \mathbf{\Lambda}]^{-1}\mathbf{\Phi}^T\mathbf{F} \tag{4}$$

with $\mathbf{Q}$ and $\mathbf{F}$ the frequency-domain realizations of $\mathbf{q}$ and $\mathbf{f}$. Note that the matrix inversion is trivial due to the diagonal nature of the equations. The frequency-domain solution to $\mathbf{x}$ can then be written as $\mathbf{X} = \mathbf{\Phi Q} = \mathbf{HF}$ where $\mathbf{H}$ is the transfer function given by

$$\mathbf{H} = \mathbf{\Phi}[-\omega^2\mathbf{I} + i\omega\bar{\mathbf{C}} + \mathbf{\Lambda}]^{-1}\mathbf{\Phi}^T \tag{5}$$

The frequency response $\mathbf{X}$ due to an arbitrary random excitation $\mathbf{F}$ cannot be uniquely specified. Instead, the response is quantified using the (PSD) of $\mathbf{X}$, $\mathbf{S}_{xx}$

$$\mathbf{S}_{xx} = \mathbf{X}\mathbf{X}^* = \mathbf{H}\mathbf{S}_{ff}\mathbf{H}^* \tag{6}$$

where the $()^*$ operator denotes the Hermitian transpose. Integrating the PSD across the frequency axis yields the variance of the response, and taking the square root of the variance yields the standard deviation. The objective function for the optimization is the maximum standard deviation of the response at any location on the beam.

The values shown in Table 1 along with a random force with a flat PSD ceiling of $1 \cdot 10^{-7}\mathrm{MPa}^2/\mathrm{Hz}$ over 0 to 1000 Hz were used for linear optimization. MATLAB's *fmincon* routine, which finds the minimum of a multivariable function subject to constraints on the inputs, was used to obtain an optimum support location of $r = 35.43\%$. A plot of displacement standard deviation against support location is shown in Figure 3. The maximum response standard deviation for this support location is 0.108 mm; for the given beam thickness of 2 mm, the beam remains in the linear response regime.

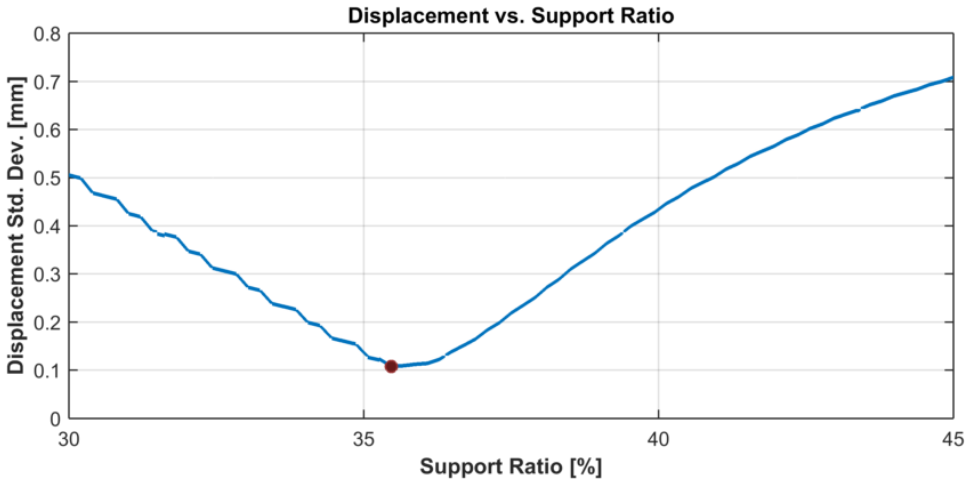

Figure 3: *A schematic of the beam under consideration for the present study.*

3 NONLINEAR MODEL DEVELOPMENT

Development of the nonlinear model consists of three main steps: Specification of a nonlinear reduced order model, development of a full-order "truth" solution for comparison, and validation. Each of the steps are described in turn below.

3.1 Nonlinear Reduced Order Models

As load levels are increased, beam deflections begin to exceed one beam thickness. At and above this level, significant nonlinearities are evident in the response. A linear analysis will significantly overestimate both the resulting deflection and stresses in the beam. It is possible to integrate the full-order finite element model in the FEM software to compute the response to a random load, however, the computational costs are many orders of magnitude higher than for the frequency domain analysis used for a linear system. The previously mentioned NLROM technique[11] can be used to reduce the computational cost while maintaining the accuracy of a nonlinear model. A nonlinear stiffness term, $\mathbf{f}_{nl}(\mathbf{x})$, is added to the linear model

$$\mathbf{M}\ddot{\mathbf{x}} + \mathbf{C}\dot{\mathbf{x}} + \mathbf{K}\mathbf{x} + \mathbf{f}_{nl}(\mathbf{x}) = \mathbf{f} \tag{7}$$

The structure is transformed to modal space using a subset of m modes

$$\ddot{\mathbf{q}} + \bar{\mathbf{C}}\dot{\mathbf{q}} + \mathbf{\Lambda}\mathbf{q} + \theta(\mathbf{q}) = \mathbf{\Phi}^T\mathbf{f} \tag{8}$$

with $\theta(\mathbf{q})$ the modal counterpart to the physical stiffness nonlinearity. This behavior can be realized using a combination of quadratic and cubic polynomials in the modal coordinates - an approach justified by use of the Green-Lagrange strain measure as applied to beams and plates in bending [17]. The r^{th} term in the nonlinear restoring force is written as follows:

$$\theta_r(q_1, q_2, ..., q_m) = \sum_{i=1}^{m}\sum_{j=1}^{m} B_r(i,j)q_i q_j + \sum_{i=1}^{m}\sum_{j=1}^{m}\sum_{k=1}^{m} A_r(i,j,k)q_i q_j q_k \tag{9}$$

The arrays A_r and B_r contain quadratic and cubic stiffness coefficients of the nonlinear model; specification of these coefficients forms the essence of the NLROM. Several approaches exist to perform this task; that used here is the Implicit Condensation and Expansion (ICE) method [18], in which a series of static loads are applied to the full order model, each one having the shape

$$\mathbf{f} = c_r M \phi_r \tag{10}$$

with a separate scaling term c_r for each mode in the basis. Were the system linear, this would cause a deformation in the r^{th} mode only. Due to the nonlinearity, however, the applied force excites a response in other modes of the structure. Kuether, Brake, and Allen[19] showed that an effective rule of thumb for selecting force amplitudes c_r is to scale them such that the nonlinear

static FE solution deflects 15 to 20 percent less (more) than a purely linear static solution due to the hardening (softening) characteristic of the nonlinearity. Combinations of up to three modal forces are applied to the full-order model, exercising all of the nonlinear modal couplings. Then, the nonlinear response of the structure is obtained from the FE software. This response is used to form a least squares problem in terms of the stiffness coefficients, which is solved to find the required coefficients.

Equation 9 features inherent coupling between the normal modes. To isolate the effects of nonlinear stiffening from those of nonlinear energy transfer, it is possible to approximate the nonlinear force expression $\theta_r(\mathbf{q})$ as

$$\theta_r(q_1, q_2, ..., q_m) = B_r q_r^2 + A_r q_r^3 \tag{11}$$

This is equivalent to collecting a set of single-mode NLROMs into an uncoupled, nonlinear dynamic system. Note that the implicit coupling between bending and membrane modes is still present; it is only the coupling between bending modes that is lost.

3.2 Full-Order Computations

Numerous techniques exist for validating NLROM's. Since the nonlinearity appears in the static stiffness terms only, a simple first check can be made by checking the static deflection of the beam to a given load; this allows easy comparison with the full-order model. A more representative check involves comparing a transient response history of the full-order and reduced-order models. A more universal (independent of loading and initial conditions) picture of the dynamics is obtained through the use of nonlinear normal modes (NNMs)[15], which depict the frequency of the structure's periodic motion as a function of energy. The NNMs are independent of the loading, and yet they are tightly connected to the transient and forced response, providing an excellent means of comparing two NLROMs. They also provide insight into the dynamics that each ROM captures, i.e. to what extent the nonlinearity causes "stiffening" or "softening" of the linear modes[20]. A comparison of NNM's is performed in Section 3.3.

For steady-state random response, however, the ideal comparison is another steady-state random response. While expensive to compute, it allows simultaneous verification of the structural model and the integration technique used, both of which will dramatically impact the results obtained. Abaqus® finite element software was used to perform such a full-order simulation. The model was discretized using 50 3-node quadratic Euler-Bernoulli beam elements (B32 in Abaqus nomenclature) which include membrane stretching effects for large displacements.

Abaqus features two direct integration methods: "Abaqus/Standard" is the traditional solver, which features an implicit Hilber-Hughes-Taylor (HHT, also "α-method") integrator[21]. The HHT integrator is a generalization of the Newmark method with the capability of adjustable numerical damping. While the Newmark method allows specification of two independent numerical parameters γ_n and β_n, behavior of the HHT method is specified by a single parameter α_n with $-\frac{1}{3} \leq \alpha_n \leq 0$; $\alpha_n = -\frac{1}{3}$ corresponds to maximum numerical damping, while $\alpha_n = 0$ corresponds to no numerical damping - this last case is also referred to as the "average acceleration" method. The Newmark parameters γ_n and β_n are related to α_n as $\gamma_n = \frac{1}{2}(1 - 2\alpha_n)$ and $\beta_n = \frac{1}{4}(1 - \alpha_n)^2$.

The HHT method is unconditionally stable with a displacement error of $O(\Delta t^2)$[22]. The availability of numerical damping, which applies in addition to any physical damping present in the model, is useful in structural dynamics problems to reduce high-frequency activity in the model that causes an automatic time-stepping routine to dramatically cut the time step. In most cases, the high-frequency activity is simply numerical noise due to the adjustment of the time step. The default setting in the Abaqus/Standard dynamic solver is $\alpha_n = -0.05$ for slight numerical damping. It is also possible to manually specify a value of α = 0 to eliminate numerical damping in the procedure. This results in a significantly longer integration time, but avoids the numerical damping of higher modes.

Abaqus also features Abaqus/Explicit, an explicit dynamic solver which uses the central difference rule for integration. Several factors make the explicit integrator attractive for high speed, nonlinear dynamics: It uses a diagonal mass matrix which allows trivial inversion to compute accelerations, it requires no iterations for accuracy, and it does not require a tangent stiffness matrix. The key disadvantage of the explicit method is its conditional stability, with a time step requirement of

$$\Delta t \leq \frac{2}{\omega_{max}} \left(\sqrt{1 + \zeta^2} - \zeta \right) \tag{12}$$

where ω_{max} is the highest natural frequency in the model and ζ the damping in that mode. Whereas the implicit integration technique is characterized by relatively large timesteps that each take a significant amount of time to compute, the explicit

technique is characterized by extremely small timesteps (often below $1 \cdot 10^{-7}$s for models requiring any type of stress fidelity) which take an insignificant amount of time to compute. Explicit methods are not often applied to problems in structural dynamics, but can be used for the problem at hand with no re-configuration of the finite element model.

It is not possible to specify modal damping parameters for general full-order problems. In Abaqus, the simplest way to apply damping to a model is through the use of mass and stiffness-proportional damping matrices, i.e.

$$\mathbf{C} = \alpha\mathbf{M} + \beta\mathbf{K} \tag{13}$$

The modal transformation then causes the modal damping matrix $\bar{\mathbf{C}}$ to become diagonal. The mass term α contributes to damping at low frequencies, while the stiffness term β contributes to damping at high frequencies. For the explicit integration routine, a non-zero β can cause extremely slow integrations due to its effect on the stable time increment. As such, only α is specified for the full-order integrations. Using a value of $\alpha = 19.54$ provides a critical damping value of $\zeta = 1\%$ at 330 Hz, near the first mode of the reference beam.

A load level of $5 \cdot 10^{-6}$ $\mathrm{MPa}^2/\mathrm{Hz}$ was specified over the frequency band of 0 to 1000 Hz, for an overall RMS of 70.7 kPa. This was sufficient to induce induce nonlinear displacements in the reference beam. The structure was integrated over a five second period at a minimum sample rate of 16 kHz (the actual sample rate for each run was, in general, much higher - see Table 2) with three different techniques: Implicit with default settings, implicit with $\alpha_n = 0$, and explicit. Using displacement at a single node (corresponding to $x = 44.29$ mm, approximately midway between the left and intermediate supports), as a metric, the three integrations are compared in Figure 4.

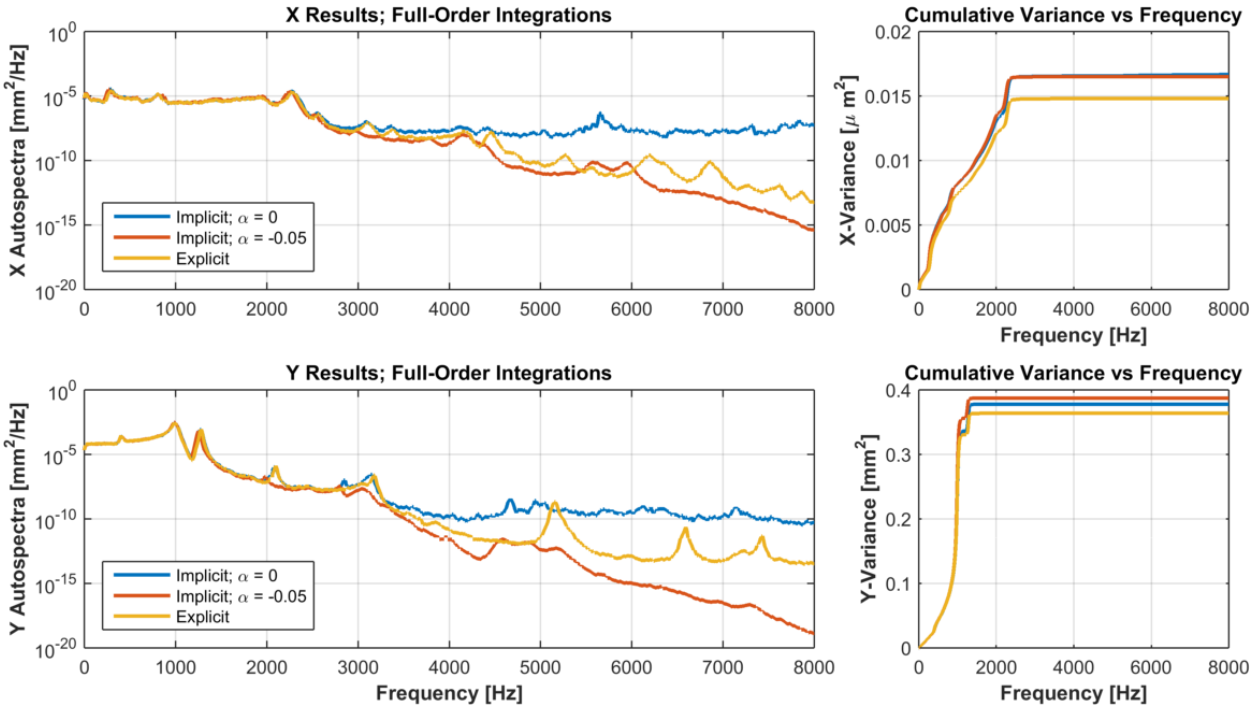

Figure 4: *Displacement at $x = 44.29$ mm of the beam using Abaqus/Standard (implicit) and Abaqus/Explicit integration routines.*

The response spectra agree well up to roughly 2000 Hz, after which the results diverge. The plots on the right-hand side of Figure 4 show, however, that the variance differences occur in the first few modes, with the implicit solutions showing displacement variance roughly 10% higher than the explicit solution. The higher-frequency peaks are so low that they contribute negligibly to the overall variance. This does not mean, however, that the high-frequency response is unimportant. Indeed, this example shows the importance of high-frequency dynamics as a mechanism for nonlinear interactions between the modes.

In the implicit case with numerical damping, high-frequency dynamics are suppressed, and the lower modes are apparently

unable to transfer energy to teach other by means of high-frequency axial deformations. As a result, the lower mode response levels are overpredicted. The implicit case without numerical damping does not suppress the high-frequency dynamics, but it also seems to obtain inaccurate results above roughly 4 kHz: the autospectrum profile resembles a flat noise spectrum rather than the response of a structure. In contrast, the explicit solver shows well-defined dynamic behavior over the entire observed spectrum, in addition to lower levels of response variance. For the remaining comparisons in this study, the Abaqus/Explicit results are used as "truth" data.

These results demonstrate that care must be taken to accurately model high-frequency dynamics and obtain an accurate response, even in a full-order model. As a consequence, the already-expensive time integration grows even more computationally intensive. Table 2 describes the total integration time for each method. Simulations were performed on four Intel i7-2600 CPU's, each with a clock speed of 3.4 GHz; 12 GB of RAM were available and the computations were not bottlenecked by memory restrictions.

	Implicit; $\alpha_n = -0.05$ [default]	Implicit; $\alpha_n = 0$	Explicit
Time	2 hours, 53 min	16 hours, 46 min	6 hours, 38 min
Increments	80,006	274,285	179,480,825

Table 2: *Simulation times and increment counts for the implicit and explicit runs, integrated for a random load over a period of five seconds.*

3.3 NLROM Creation and Validation

With a full-order model and its associated random response solutions obtained, NLROM validation can take place. An NLROM including the first five modes of the structure was used for all of the following computations. In constructing the NLROM, load levels causing a 50% thickness displacement in each mode were sufficient to meet the nonlinear activation criteria mentioned in Section 3.1. (At a displacement of 50% the beam thickness, the nonlinear response was approximately 80% of the linear response for each mode). Both a fully-coupled NLROM (as per (Equation 9)) and a diagonalized NLROM (Equation (11)) are used in the validation plots below.

The NNMs of the coupled and uncoupled NLROMs were computed in order to examine any immediate differences between the two nonlinear models. A frequency-energy plot of the comparison is shown in Figure 5. The "backbone" curves of the two models are very similar, however, there is an internal resonance visible in the NNM of the coupled NLROM, which corresponds to an interaction between the first and fourth normal modes of the structure.

Next, the direct integration results are compared to further evaluate the NLROMs. Each model was integrated in MATLAB using a fixed time-step HHT routine with no numerical damping. An integration sample rate of 48 kHz was necessary to achieve convergence with the Abaqus results. (The average sampling rate that each Abaqus routine used can be inferred from Table 2.) Figure 6 compares the NLROMs with Abaqus/Explicit results using the vertical displacement at a single node of the beam. The coupled NLROM matches Abaqus very well; the diagonal NLROM proves to be surprisingly accurate, although it does overpredict the response by 15% relative to the full-order solution. Note that the result for the linear case with this loading yields an RMS response of 0.76 mm, more than twice the nonlinear solution.

The stresses in the various models were also compared over all of the integration points in the full-order model (the stress at these locations is available from the ROMs). In Figure 7, contour plots of stress are shown as functions of position vs. frequency. At right, the standard deviation and mean of the stress fields are compared. The largest differences in the stress autospectra are seen in the higher frequencies; for example, near 2000 and 3000 Hz, the diagonal NLROM predicts peak stress near the linear natural frequencies, whereas the other two models predict that these frequencies stiffen due to the large response of the lower frequency modes. This presumably causes the peak stress, near 1000 Hz, to be too large in the diagonal NLROM.

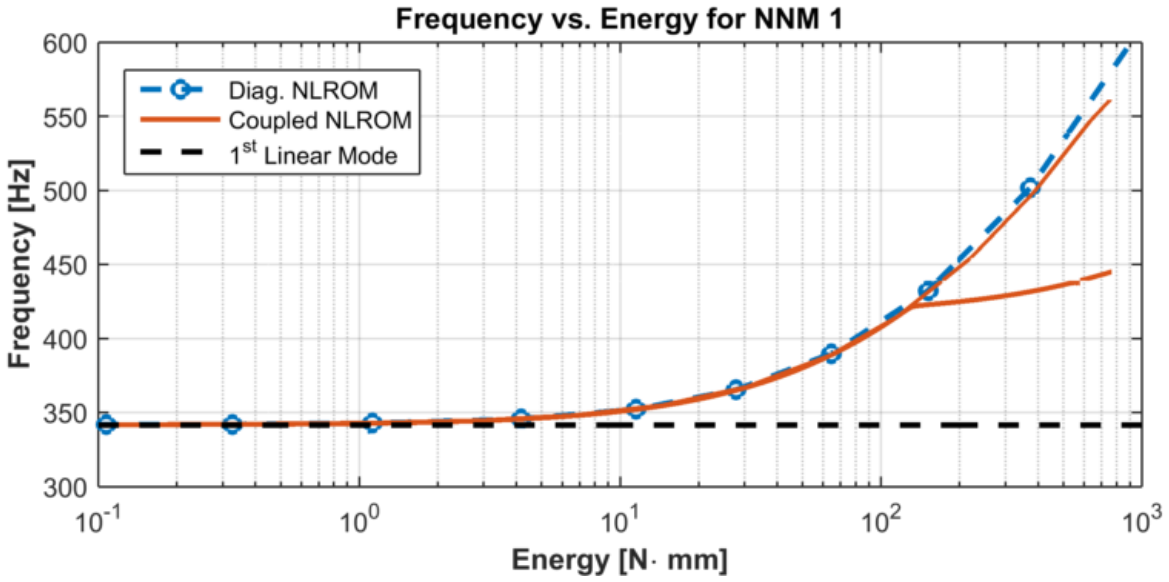

Figure 5: *Comparison of the beam's 1st NNM computed from a coupled 5-mode NLROM and an uncoupled NLROM.*

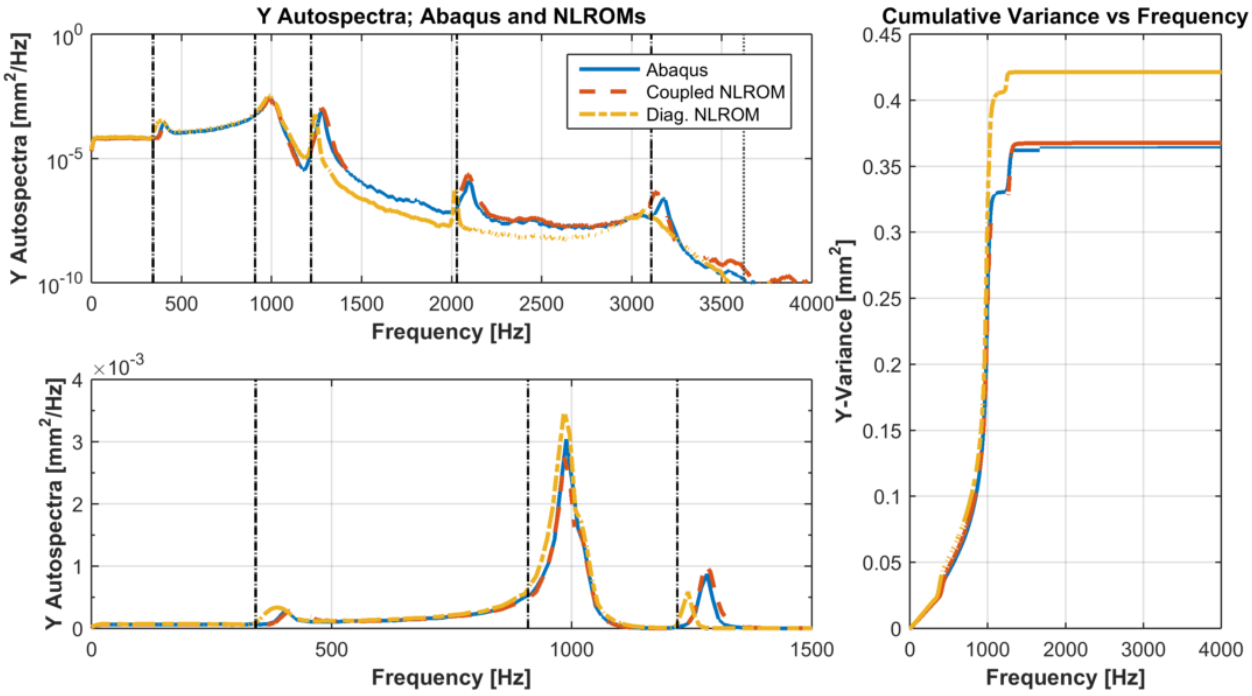

Figure 6: *Displacement at $x = 44.29$ mm of the beam using Abaqus/Explicit results, a coupled five mode NLROM, and a diagonal five mode NLROM. Vertical dash/dot lines correspond to linear natural frequencies of modes included in the NLROM; dotted lines indicate linear natural frequencies of modes not included in the NLROM. Top Left: Log scale response PSD. Right: Cumulative response variance. Bottom Left: Linear scale response PSD zoomed to show three lowest modes.*

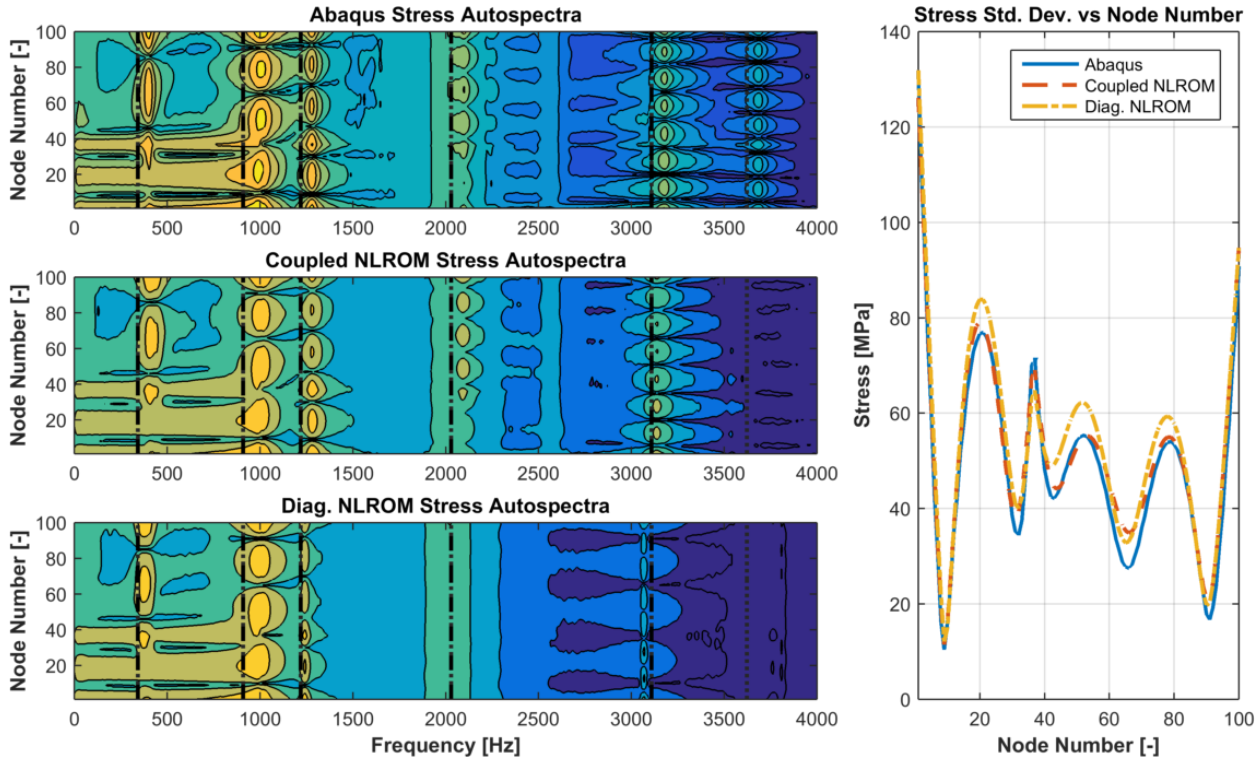

Figure 7: *Stress autospectra of the beam at all element integration points (left) and the resulting standard deviation (right) levels using Abaqus/Explicit results, a coupled five mode NLROM, and a diagonal five mode NLROM. Vertical dash/dot lines correspond to linear natural frequencies of modes included in the NLROM; dotted lines indicate linear natural frequencies of modes not included in the NLROM.*

4 PARAMETER SWEEP

Once the reduced order models were obtained and validated, a two-dimensional numerical parameter sweep was performed. This technique is not generally applicable to optimization problems due to its high computational cost, but in this study it is valuable because it provided a view of how displacement and stress varied over a wide parameter range. The modified parameters were the uniform thickness of the beam t and the location of the support given by the ratio r, over the range $1.5 \text{ mm} \leq t \leq 3.5 \text{ mm}$ and $25\% \leq r \leq 40\%$. 20 thickness values and 18 support locations were simulated, for a total of 360 points in the grid. Each point took roughly two minutes to compute between NLROM construction, time integration, and stress extraction.

Figure 8 shows the results for the coupled NLROM. the maximum root mean square (RMS) values of stress and displacement are shown for each configuration. With full time histories available for each response, condensation into the RMS value is not necessarily the best choice of objective function. For example, a designer might be more interested in the estimated lifetime of the component, and substitute the results into a fatigue-life estimation routine; one might also use the results to estimate the likelihood of exceeding a certain threshold. (The non-Gaussian nature of the nonlinear response complicates this task). The RMS value is used here purely for its simplicity.

First, examine the coupled contours in Figure 8. At high beam thicknesses, both stress and displacement contours show that the optimal design tends towards the support location at 34%, which was the linear optimum. As the thickness of the beam decreases and the response enters the nonlinear regime, the optimal location for minimum stress shifts markedly leftward, while the optimal location for minimum displacement remains essentially unchanged. Increases in thickness seem to lead to monotonic decreases in stress, again as would be expected for a linear optimization. The topology of the response is, at large scales, smooth and convex, with no observable local minima. This suggests that, for nonlinear stiffening structures in a random load environment, any number of traditional stochastic optimization techniques could be appropriate, and global optimization techniques (e.g. a genetic algorithm, particle swarm optimization, etc.) need not be applied. Future work will explore the applicability of common

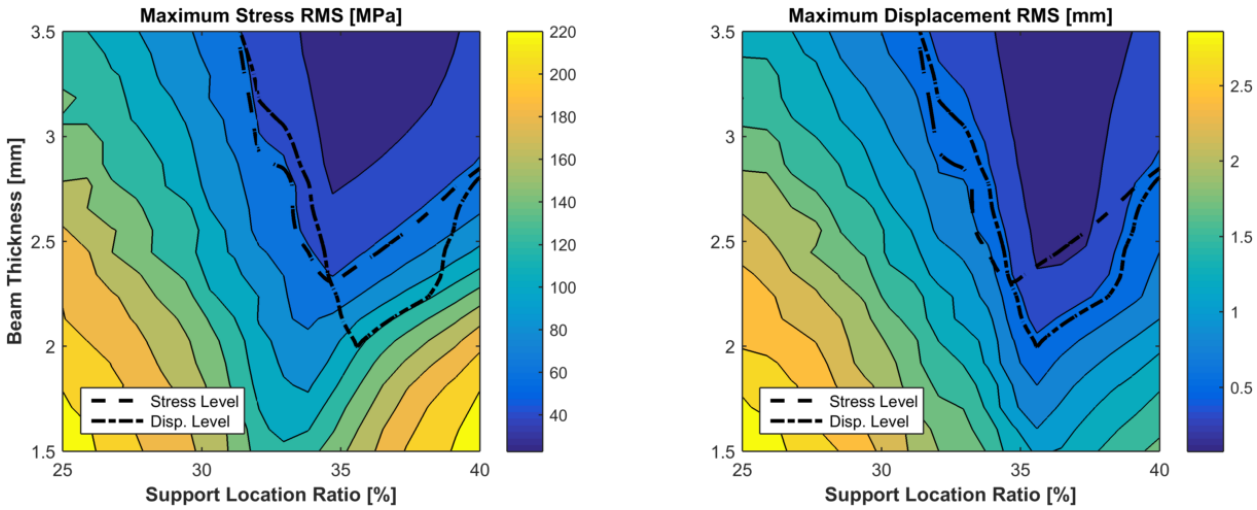

Figure 8: *Stress and displacement contours for five-mode coupled NLROM. Dashed and dash/dot lines indicate RMS displacement of 0.7 mm and RMS stress of 65 MPa.*

stochastic optimization techniques, such as the use of response surface methods or stochastic finite differences.

The parameter sweep results can be used to perform a representative optimization through the use of interpolating contours. Consider the problem of minimizing thickness with constraints on stress and displacement. Contours of level stress and displacement can be inscribed on the $t-r$ plane as in Figure 8 for a displacement RMS of $\delta = 0.7\text{mm}$ and a stress RMS of $\sigma = 65MPA$, such that the minimum-thickness design which meets the constraints can be found at $t = 2.33$ mm, $r = 34.6\%$.

Now consider the diagonal contours in Figure 9. For ease of comparison, the results of the diagonal NLROM are shown in terms of departure from the coupled NLROM, with positive values of stress and displacement standard devation corresponding to a higher prediction of the diagonal NLROM. Absolute difference, rather than percentage difference, is used in order to mitigate further noise in the (already quite noisy) results.

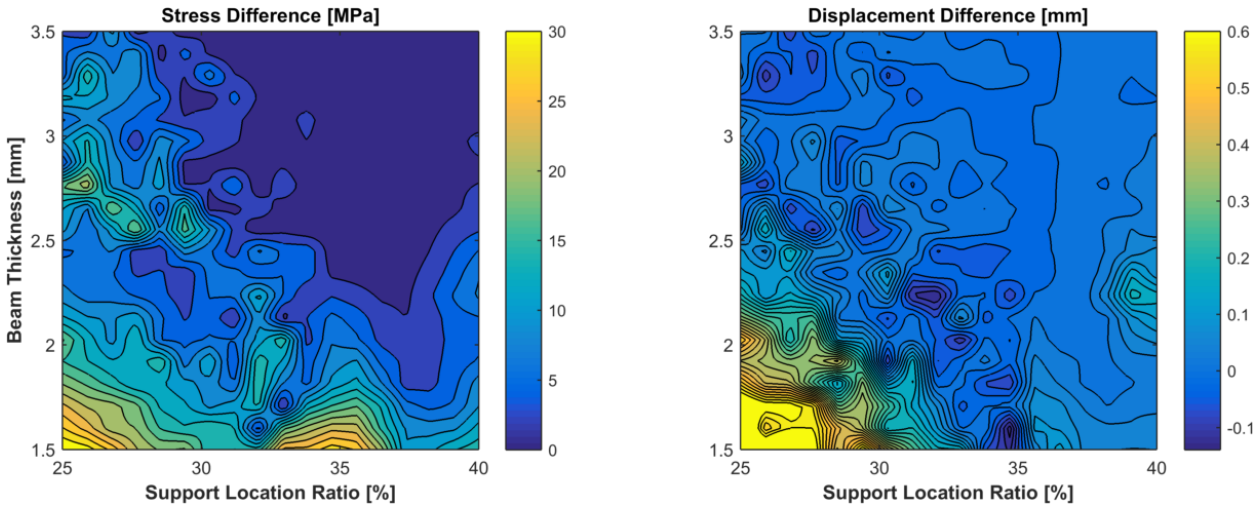

Figure 9: *Stress and displacement contours of the five-mode diagonal NLROM in terms of a departure from the five mode coupled NLROM.*

Unfortunately, no clear narrative on the effect of modal energy transfer emerges from these plots. Variations in the stress and displacement fields are too large to be caused by sampling error from the response statistics, but follow no discernible pattern based on the configuration of the beam. As the support location is shifted leftward and the thickness lessened, the overal stiffness of the beam is reduced and energy transfer effects become more apparent. The highest levels of energy transfer seen in the configuration space occur at the bottom left corner of the plot. Re-simulating this configuration in Abaqus/Explicit and in MATLAB using each NLROM leads to the displacement autospectrum plot of Figure 10.

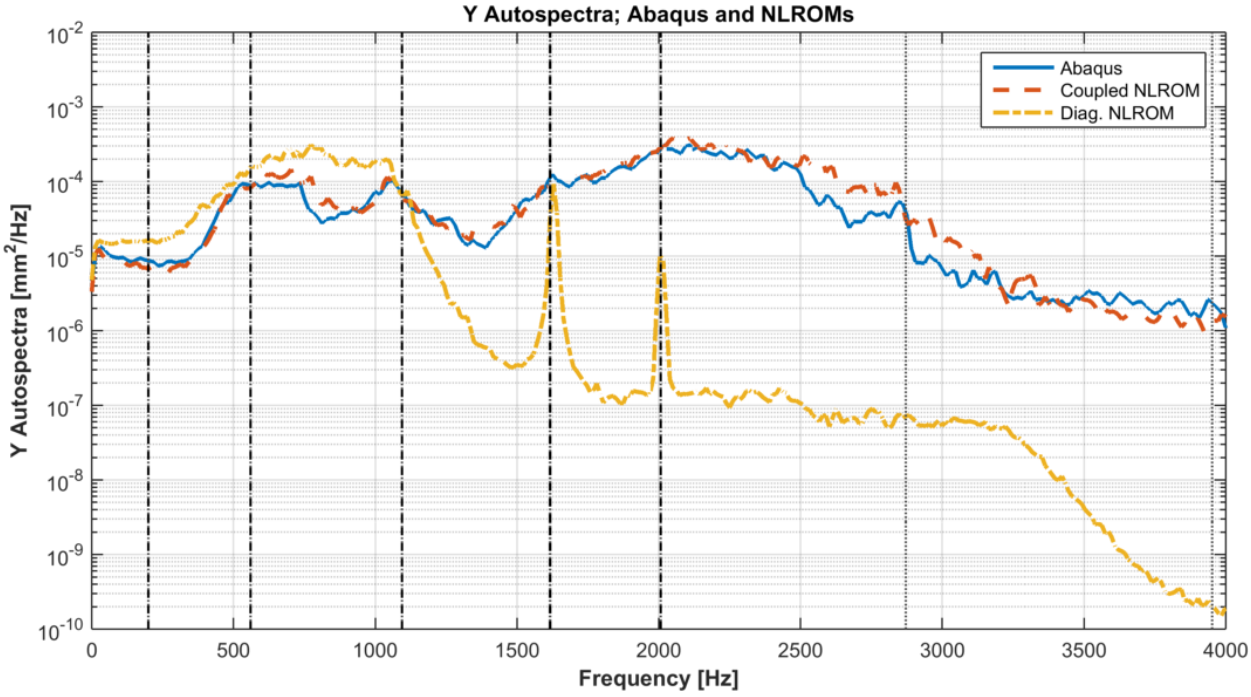

Figure 10: *Displacement at $x = 44.29$ mm of the beam using Abaqus/Explicit results, a coupled five mode NLROM, and a diagonal five mode NLROM. Vertical dash/dot lines correspond to linear natural frequencies of modes included in the NLROM; dotted lines indicate linear natural frequency of modes not included in the NLROM.*

This location does not correspond to the maximum displacement point of the beam, but still provides insight into the dynamics in play: The Abaqus/Explicit and coupled NLROM results have degenerated into a nearly flat response across the frequency spectrum, with significant activation of modes lying outside the 1000 Hz forcing bandwidth. The uncoupled NLROM, on the other hand, drops off in response immediately after 1000 Hz, with modes above this level behaving in a linear manner. This is exactly the large-scale energy transfer behavior that is of interest, however, the response of the structure at this load level is too high to be of practical use.

5 CONCLUSION

The effect of modal energy transfer normal modes was examined in the context of a flat beam structure with a variable configuration. While generating truth data through direct integration of the full finite element model, the importance of energy transfer was indirectly demonstrated by varying the parameters of a full-order finite element integration; different procedures and settings yielded significantly different displacement statistics due to the suppression of high-frequency membrane effects through numerical damping, producing response errors on the order of 10%. Since the power transferred to a mode is a product of the applied force and the modal velocity, it seems that if the high frequency modes are suppresed by numerical damping, they cannot absorb as much power from the low frequency modes. As a result, the response amplitude at low frequencies is over-predicted.

The requirement to include such high-frequency effects also demonstrates the futility of random response and other long-time-history prediction through full-order simulation: Not only are long time histories required, but extremely small time increments are

necessary to accurately predict nonlinear response. In this case, the explicit integration method, often considered too expensive for structural dynamics problems, had the best combination of accuracy and efficiency relative to the Newmark/HHT method with no numerical damping.

To obtain a quantitative understanding of the effects of modal energy transfer across multiple configurations of the beam, two sets of nonlinear reduced order models were developed: The first featured a full set of modal coupling terms between the modes, while the second was "diagonalized" and featured quadratic and cubic terms of single modes only. Comparing the displacement, energy, and stress results of these two NLROMs at a single design point showed that, as expected, the coupled NLROM closely matched full-order Abaqus results, while the diagonalized ROM overpredicted both stress and displacement levels. Using the efficient analysis capabilities of the NLROMs, a grid of 360 design points was evaluated for maximum stress and displacement RMS over a 7.5 second time history. This "parameter sweep," though not an effective means of optimization in general, provided a general overview of the topology of this type of design space, showing largely convex behavior without the prevalence of local minima that would require a global optimization technique.

Finally, the difference in response between the coupled and diagonal NLROMs was investigated. For this structure, no discernible pattern or preferential behavior was observable in the response contours. Examining a single solution for which nonlinear energy transfer was a major factor did show the prevalence of modal interaction in that particular example, but was at too high a response level to be of any practical use. The results here are inconclusive as to the feasibility of leveraging nonlinear energy transfer within a structure to reduce the response levels. A key difficulty in attempting to maximize the internal energy transfer within a structure is that the primary mechanism governing the transfer seems to be the ratios between linear natural frequencies; there is no apparent method to modify these natural frequency ratios without also modifying the stiffness of the structure with respect to a dynamic forcing. In this case, modifying the natural frequency ratios by shifting the support also led to a reduction in overall stiffness as the support moved away from the 34% location corresponding to maximum bending stiffness.

Future work on this topic will include a consideration of applicable optimization techniques for the nonlinear random response problem and evaluation of substructuring and reduced order modeling techniques for more complex, built-up structures. A similar investigation of energy transfer effects in curved structures, which exhibit stronger coupling between axial and bending modes, is also of interest. A less computationally-intensive and more exact method of quantifying energy transfer between a structure's modes will also be examined.

Overall, the use of nonlinear analysis techniques for design optimization shows great promise in terms of achievable weight reduction for a given set of constraints on stress and displacement. Modal interactions in nonlinear structures are still not well understood, but it is clear from this and other studies that they play a key role in nonlinear dynamic response. Even if it is not possible to target high energy transfer levels as a design goal, they still enable the reduction of a nonlinear response by sending energy outward from excited modes to those out of the excitation bandwidth; a behavior which can be either benficial or detrimental. An understanding of these effects will be invaluable in the pursuit of efficient nonlinear structures.

ACKNOWLEDGMENTS

This material is based upon work supported by the National Science Foundation Graduate Research Fellowship under Grant No. DGE-1256259. Any opinion, findings, and conclusions or recommendations expressed in this material are those of the authors(s) and do not necessarily reflect the views of the National Science Foundation.

The authors also acknowledge Joseph Hollkamp from the Air Force Research Laboratory's Structural Sciences Center, for the insights that he shared and for providing the Abaqus interface that was used in this work.

References

[1] R. W. Gordon and J. J. Hollkamp, "Reduced-order models for acoustic response prediction," Tech. Rep. AFRL-RBWP-TR-2011-3040, Air Force Research Laboratory, 2011.

[2] N. Teunisse, P. Tiso, L. Demasi, and R. Cavallaro, "Computational reduced order methods for structurally nonlinear joined wings," in *56th AIAA/ASCE/AHS/ASC Structures, Structural Dynamics, and Materials Conference*, (Kissimmee, Florida), January 2015.

[3] J. Wang, C. Tzikang, D. W. Sleight, and A. Tessler, "Simulating nonlinear deformations of solar sail membranes using explicit

time integration," in *45th AIAA/ASCE/AHS/ASC Structures, Structural Dynamics, and Materials Conference*, (Palm Springs, California), March 2004.

[4] E. J. Tuegel, A. R. Ingraffea, T. G. Eason, and M. S. Spottswood, "Reengineering aircraft structural life prediction using a digital twin," *International Journal of Aerospace Engineering*, vol. 2011, 2011.

[5] M. Nash, *Nonlinear Structural Dynamics by Finite Element Modal Synthesis*. PhD thesis, Department of Aeronautics, Imperial College, 1977.

[6] D. J. Segalman and C. R. Dohrmann, "Method for calculating the dynamics of rotating flexible structures, part 1: Derivation," *Journal of Vibration and Acoustics, Transactions of the ASME*, vol. 118, pp. 313–317, 1996.

[7] D. J. Segalman and C. R. Dohrmann, "Method for calculating the dynamics of rotating flexible structures, part 2: Example calculations," *Journal of Vibration and Acoustics, Transactions of the ASME*, vol. 118, pp. 318–322, 1996.

[8] M. I. McEwan, J. Wright, J. E. Cooper, and A. Y. T. Leung, "A combined modal/finite element analysis technique for the dynamic response of a non-linear beam to harmonic excitation," *Journal of Sound and Vibration*, vol. 243, pp. 601–624, 2001.

[9] A. A. Muravyov and S. A. Rizzi, "Determination of nonlinear stiffness with application to random vibration of geometrically nonlinear structures," *Computers and Structures*, vol. 81, pp. 1513–1523, 2003.

[10] M. P. Mignolet, A. Przekop, S. A. Rizzi, and S. M. Spottswood, "A review of indirect/non-intrusive reduced order modeling of nonlinear geometric structures," *Journal of Sound and Vibration*, vol. 332, pp. 2437–2460, 2013.

[11] J. J. Hollkamp, R. W. Gordon, and S. M. Spottswood, "Nonlinear modal models for sonic fatigue response prediction: a comparison of methods," *Journal of Sound and Vibration*, vol. 284, pp. 1145–1163, 2005.

[12] D. Suguang and J. S. Jensen, "Optimization of nonlinear structural resonance using the incremental harmonic balance method," *Journal of Sound and Vibration*, vol. 334, pp. 239–254, 2015.

[13] C. Grappasonni, G. Habib, T. Detroux, F. Wang, G. Kerschen, and J. S. Jensen, "Practical design of a nonlinear tuned vibration absorber," in *International Conference on Noise and Vibration Engineering*, (Leuven, Belgium), September 2014.

[14] J. D. Schoneman and M. S. Allen, "Leveraging geometric nonlinearity for efficient design of thin beams," in *57th AIAA/ASCE/AHS/ASC Structures, Structural Dynamics, and Materials Conference*, (San Diego, CA), 2015. Forthcoming.

[15] G. Kerschen, M. Peeters, J. Golinval, and A. F. Vakakis, "Nonlinear normal modes, part i: A useful framework for the structural dynamicist," *Mechanical Systems and Signal Processing*, vol. 23, no. 1, pp. 170–194, 2009.

[16] A. H. Nayfeh, *Introduction to Perturbation Techniques*. John Wiley & Sons, 2011.

[17] J. B. Rutzmoser and D. J. Rixen, "Model order reduction for geometric nonlinear structures with variable state-dependent basis," *Dynamics of Coupled Structures*, vol. 1, pp. 455–462, 2014.

[18] J. J. Hollkamp and R. W. Gordon, "Reduced-order models for nonlinear response prediction: Implicit condensation and expansion," *Journal of Sound and Vibration*, vol. 318, pp. 1139–1153, 2008.

[19] M. S. Allen, R. J. Kuether, B. Deaner, and M. W. Sracic, "A numerical continuation method to compute nonlinear normal modes using modal reduction," in *53rd AIAA/ASCE/AHS/ASC Structures, Structural Dynamics, and Materials Conference*, (Honolulu, Hawaii), 2012.

[20] R. J. Kuether, M. R. Brake, and M. S. Allen, "Evaluating convergence of reduced order models using nonlinear normal modes," *Model Validation and Uncertainty Quantification*, vol. 3, pp. 287–300, 2014.

[21] Dassault Systems Simulia Corp., *Abaqus Theory Manual*, 2012.

[22] R. D. Cook, D. S. Malkus, M. E. Plesha, and R. J. Witt, *Concepts and Applications of Finite Element Analysis*. 4 ed.